Renewable Energy 180 (2021) 966–979

Contents lists available at ScienceDirect

Renewable Energy

journal homepage: www.elsevier.com/locate/renene

Subsurface utilization as a heat sink for large-scale ground source heat pump: Case study in Bangkok, Thailand

Yutaro Shimada [a, *], Koji Tokimatsu [a], Takashi Asawa [a], Youhei Uchida [b], Akira Tomigashi [b], Hideaki Kurishima [c]

[a] School of Environment and Society, Tokyo Institute of Technology, 4259 Nagatsuta-cho, Midori-ku, Yokohama, Kanagawa, 226-8503, Japan
[b] Renewable Energy Research Center, National Institute of Advanced Industrial Science and Technology, 2-2-9 Machiikedai, Koriyama-shi, Fukushima, 963-0298, Japan
[c] School of Architecture, Shibaura Institute of Technology, 3-7-5 Toyosu, Koto-ku, Tokyo, 135-8548, Japan

ARTICLE INFO

Article history:
Received 5 May 2021
Received in revised form
5 August 2021
Accepted 29 August 2021
Available online 3 September 2021

Keywords:
Ground source heat pump
Energy saving
Tropical region

ABSTRACT

Subsurface utilization in the tropical regions as a heat sink for ground source heat pumps (GSHPs) leads to thermal buildup in the long term, resulting in the decreased energy performance. However, the applicability of the GSHP in these regions has never been investigated based on the predicted heat sink temperature over a lifetime. This study aimed to evaluate the energy performance of a large-scale GSHP system in representative building models in Thailand based on operating conditions derived from a predicted 50-year heat sink temperature. The proposed system combines a GSHP and an air-source heat pump (ASHP), and, in one scenario, the GSHP also supplies hot water. The results confirm that the combined system achieves a higher efficiency than that of an ASHP system alone, and GSHP supplying hot water realizes substantial energy-saving. However, limitations on the annual GSHP operation hours are essential, resulting in low energy-saving performance for cooling dominated facilities. Further improvements are expected by mitigating the thermal interactions among each borehole heat exchanger.

1. Introduction

In recent years, the demand for space cooling has increased, and continues to grow in tropical regions owing to rapid economic development. The International Energy Agency forecasts that stocks of air-conditioning units in association of southeast Asian nations (ASEAN) countries, which are located in the tropics, will increase from approximately 40 million units in 2018 to 350 million in 2040 [1]. This demand increase would cause an increase in peak power, power consumption, and consequent CO_2 emissions, making it necessary for air conditioners to have high energy performance.

A ground source heat pump (GSHP) is an air conditioner that uses low-grade thermal energy that is present in the shallow subsurface up to a depth of approximately 400 m (called shallow geothermal energy) [2]. Here, the subsurface temperature is constant throughout the year and is relatively lower (higher) than the outside temperature in the summer (winter) in mid- and high-latitude regions [3]. This makes the temperature gap between the refrigerant's condensation and evaporation points smaller than that in an air source heat pump (ASHP) or a conventional air conditioner that exchanges heat with the outside air. This smaller temperature gap enables the GSHP to operate with a higher energy performance than the ASHP. Specifically, a GSHP introduced in an office building in central Tokyo had an annual energy-saving rate (*AESR*) of 49%, which exceeded that of an ASHP [4].

In tropical regions, the subsurface temperature is considered to be equal to or higher than the outside temperature owing to small seasonal fluctuations in the outside temperature, leading to the consensus of a small energy-saving effect by GSHPs in these regions [5]. However, a geological survey conducted in the Chao Phraya Plain, Thailand and the Red River Plain, Vietnam revealed that the subsurface temperature up to a 50 m depth is lower than the outside temperature during the daytime in some locations [6]. In particular, in Bangkok, Thailand, the daily maximum outside temperature exceeds 35 °C from March to May, and the subsurface temperature at a depth of 20–50 m is 29–31 °C. It was reported that this phenomenon is attributable to the perturbation of the subsurface thermal regime by natural groundwater flow at both

* Corresponding author. ;
E-mail address: shimada.y.aj@m.titech.ac.jp (Y. Shimada).

https://doi.org/10.1016/j.renene.2021.08.116
0960-1481/

Abbreviations

AES	Annual energy savings
AESR	Annual energy saving rate
ASEAN	Association of southeast Asian nations
ASHP	Air-source heat pump
ASHRAE	American society of heating refrigeration and air conditioning engineers
BHE	Borehole heat exchanger
CL	Cooling load
cm	Circulation medium
COP	Coefficient of performance
cw	Chilled water
FR	Flow rate
GCV	Gross calorific value
GSHP	Ground source heat pump
HDPE	High-density polyethylene
HER	Heat exchange rate
HL	Heating load
HP	Heat pump
HVAC	Heating, ventilation, and air conditioning
ICS	Infinite cylindrical source
ILS	Infinite line source
in	Inlet
LCEM	Life cycle energy management
PSR	Power-saving rate
RMSE	Root-mean-square error
TD	Temperature difference
TL	Total length
U-value	Overall heat transfer coefficient

Symbols

a	Thermal diffusivity
c	Specific thermal capacity
E	Exponential integral
E_x	Electric power
g	Ground
j	Specific hour
q	Heating amount
r	Distance from infinite line source
t	Elapsed time
u	Variable
w	Water
λ	Ground thermal conductivity

local and regional scales. In particular, the subsurface temperature in the groundwater recharge zone was lower than that in the discharge zone at the same depth. Therefore, even in tropical regions, the shallow subsurface may be used as a heat sink in areas expecting groundwater flow.

Based on the aforementioned survey, demonstration experiments were conducted to evaluate the energy performance of small-scale GSHPs for space cooling in southeast Asian countries, such as Thailand, Vietnam, and Indonesia [7–12]. The field test in Thailand achieved a power-saving rate (*PSR*) of approximately 30% with a vertical borehole heat exchanger (BHE) as the ground heat exchanger and approximately 18% with a horizontal BHE [10,11]. Moreover, the field test data for a GSHP with a vertical BHE were analyzed. The results showed that in Bangkok, Thailand, a small-scale GSHP with a vertical BHE (total length of 65 m) was superior to an ASHP in terms of long-term energy performance [12]. However, these experiments and performance evaluations were limited to small-scale systems with a maximum cooling capacity of 4 kW, which requires only one or two vertical BHEs. While the performance of a large-scale system that requires multiple BHEs was not investigated, its heat sink temperature is expected to increase faster than that of a small-scale system owing to the thermal buildup between the BHEs. As large commercial buildings consume more than half of the electricity in the business sector in Thailand, of which approximately 60% is for space cooling, exploring the energy performance of large-scale systems is highly pertinent [13,14].

Some studies have simulated the performance of GSHP systems with multiple BHEs in regions dominated by cooling demand, finding that they achieved *AESRs* that were more than 10% greater than those of ASHP systems [15,16]. However, these studies did not impose a limitation on the GSHP operation based on the heat exchange rate and annual operation time. The tropical setting contributes a significant cooling load on buildings to maintain thermal comfort, leading to an extreme load imbalance. Intensive operation can result in a loss of superiority in energy performance before reaching a system lifetime owing to rapid increases in heat sink temperatures. Therefore, operating conditions must be set to achieve a higher efficiency than the conventional system based on the predicted heat sink temperature over the system's lifetime. Consequently, large-scale GSHPs in tropical regions may not process the entire cooling load of a building, requiring the assistance of other cooling systems, such as ASHPs.

Therefore, this study aimed to evaluate the potential of subsurface utilization in the tropics as a heat sink for large-scale GSHP systems in terms of energy performance. The *PSR* and *AESR* values for a large-scale GSHP system in combination with an ASHP system (hybrid GSHP system) were investigated for representative commercial buildings in Bangkok, Thailand. The energy consumption in the ASHP system was used as a reference performance for a conventional cooling system. The operating conditions of the GSHP system was set to achieve a higher efficiency than that of the conventional ASHP system based on the predicted heat sink temperature over the lifetime. The heat exchange rate (i.e., heat load/unit length of a borehole) with fixed annual operating hours was used as an indicator of the operating conditions. Four representative commercial buildings, including an office, school, hotel, and supermarket, were modeled differently for both the cooling demand patterns and the scale of installable ground heat exchangers. Three simulation models, DesignBuilder, the life cycle energy management (LCEM) tool, and GroundClub were coupled to simulate the operating status of the cooling system at hourly intervals. This study followed a three-step analysis:

1) Designing commercial building models and calculating the cooling loads.
2) Determining the operating conditions of the GSHP to achieve higher efficiency than the ASHP over the lifetime of the ground heat exchanger based on a predicted 50-year heat sink temperature.
3) Modeling a chilling system using both GSHP and ASHP based on the cooling load found in step 1) and the operating conditions specified in 2). Finally, the hourly power consumption of the modeled chilling system is calculated.

2. Methods

2.1. Building models and cooling load simulations

Using the building simulation software DesignBuilder v5.5 [17], we developed representative building models with a total floor area of approximately 10,000 m^2. The building geometry was designed by referring to previous studies that created reference building models for Thailand [18,19]. Fig. 1(a) shows the floor plans of the square-shaped office, hotel, and supermarket models. The interior square is divided into core and peripheral zones, in which the peripheral zone is an air-conditioned area with occupants and internal heat gains, and the core zone is a non-conditioned area without occupants and internal heat gains. In the school, the proportion of air-conditioned area to the total floor area is small. Thus, the school model's floor plan is rectangular and divided into north and south zones, as shown in Fig. 1(b), wherein the south zone is the air-conditioned area with occupants and internal heat gains, and the north zone is the non-conditioned area without occupants and internal heat gain.

The office, school, and hotel models are 10-story buildings, whereas the supermarket model is a three-story building. According to Thailand's energy audit, the air-conditioned areas of large-scale buildings, such as offices, hotels, and supermarkets, account for approximately 60%–70% of the total floor area, while that in schools account for approximately 30% [20]. Herein, we followed the energy audit, considering the percentage of air-conditioned area to be 70% for the office, hotel, supermarket, and 30% for the school. The window-to-wall ratio was 0.4 for the office, school, and hotel models, while it was 0.2 for the supermarket model. Table 1 lists the dimensions of representative building models, and Table 2 summarizes the construction materials and overall heat transfer coefficient (U-value) of each building element.

Internal heat gains associated with activities include lighting, equipment, occupants, and corresponding ventilation. We assumed that all floors inside a building were used for a single purpose in the office, school, and supermarket models. Conversely, we assumed multiple purposes in the hotel model, in which the first, second, and third through tenth floors were considered to be a lobby, restaurant, and guestrooms, respectively. We used lighting energy audit information to define the average lighting power density in each facility for business hours [20]. Meanwhile, the average equipment power density during business hours was obtained by subtracting the lighting and air conditioning energy audit information from the audit information of each facility's total energy consumption. We obtained the average occupant density and required ventilation from the American society of heating refrigeration and air conditioning engineers (ASHRAE) Standard 62.1–2019 [21] and the occupant heat gain from the ASHRAE Standard 55–2017 [22]. The indoor environment was set to a temperature of 25 °C, with a relative humidity of 50% during the business hours of each facility. Table 3 lists the internal heat gain and activity parameters.

Table 1
Dimensions of the representative building models.

Building purpose	A	B	C	Area per floor
Office, Hotel	31.6 m	17.3 m	–	998.6 m^2
Supermarket	57.7 m	31.6 m	–	3329.3 m^2
School	15.8 m	4.74 m	63.2 m	998.6 m^2

* Note: A–C in the table can be found in Fig. 1.

We used the EnergyPlus engine [23] in DesignBuilder and EnergyPlus weather data [24] to simulate the hourly cooling loads of the building models (excluding heating load due to the hot climate in Bangkok). EnergyPlus weather data were retrieved from the International Weather for Energy Calculations database, which contains weather data from the 1980s to the1990s [25]. For simplicity, we disregarded climate change and the urban heat island phenomenon. Fig. A provides the monthly averages of the maximum temperature, minimum temperature, and relative humidity retrieved from the EnergyPlus weather data.

2.2. Operating conditions of a large-scale GSHP system

2.2.1. Simulation model in GroundClub

We used the GSHP simulation software GroundClub v1.0.0.30 to reproduce the temperature response of the BHE and to derive the operating conditions for the GSHP [26–28]. This software reproduces the heat transfer in the subsurface and the temperature response around the vertical BHE by analytically solving the heat conduction equation in the cylindrical coordinate system. It can also reproduce the temperature response of multiple vertical BHEs embedded in arbitrary arrangements by superposing the temperature fields of the infinite cylindrical source (ICS) [29] and infinite line source (ILS) solutions [30]. In particular, the ICS and ILS solutions were applied to reproduce the temperature response owing to the heat flux of the considered BHE and neighboring BHEs, respectively [27,28]. GroundClub was applied for verification purposes to simulate a GSHP with eight BHEs introduced in an office building in Tokyo. The annual root-mean-square error (RMSE) was 0.65 °C between the measured inlet temperature in the heat pump and the value calculated using GroundClub [31] to confirm its high reproducibility. The analytical solutions used in this software considered the following assumptions to simplify the conditions:

a. The initial temperature distribution of the subsurface is uniform in the depth direction.
b. The soil and BHE materials have isotropically homogeneous physical and thermal properties.

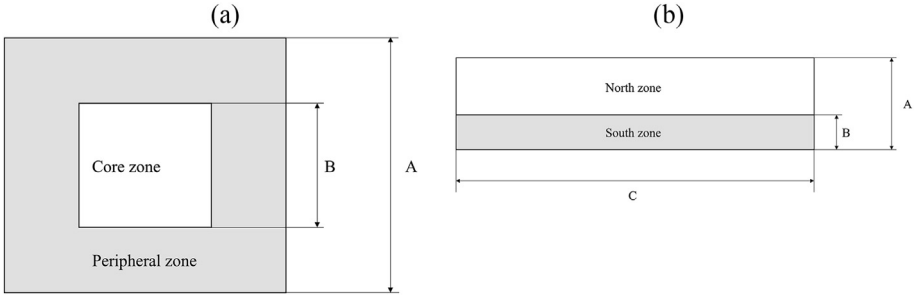

Fig. 1. Representative building model floor plans
*See Table 1 for the lengths of A – C.

Table 2
Construction materials and thermal properties of building elements.

Description	Materials	Thickness (mm)	U-value (W/(m^{2}K))
External opaque wall	Mortar	10	1.001
	Concrete block (light weight)	150	
	Plaster	10	
Roof	Cast concrete	100	0.589
	Air gap	300	
	MW glass wool	50	
	Plaster board	10	
Ground floor	Cast concrete	150	1.991
	Floor/roof screed	50	
	Ceramic floor tiles dry	30	
Internal floor	Plaster board	10	2.294
	Cast concrete	100	
	Ceramic floor tiles dry	30	
Glazing	Dbl LoE tint 6 mm/13 mm Arg (SHGC: 0.364)		1.499

*SHGC: solar heat gain coefficient.

Table 3
Internal heat gain and activity parameters identified from the literature.

Category	Office	School	Hotel (Room)	Hotel (Lobby)	Hotel (Restaurant)	Supermarket	Reference
Business hours (HVAC activity schedule)	Weekday 8:00 −17:00		All days 24 h	All days 5:00–23:00	All days 6:00–21:00	All days 10:00–22:00	[21,24]
Occupant density (person/100 m^2)	5	35	10	30	70	8	[22]
Occupant heat gain (W/person)	117	108	117	126	117	180	[23]
Ave. Equipment power density (W/m^2)	14	18	2.7			37.9	Own calc.
Ave. Lighting power density (W/m^2)	11.6	8.2	4			18.7	Own calc.
Fresh air ventilation (l/s-person)	2.5	5	2.5	3.8	3.8	3.8	[22]
Mechanical ventilation (l/s-m^2)	0.3	0.6	0.3	0.3	0.9	0.3	[22]

c. Heat is transferred only by conduction.

2.2.2. Operating conditions based on long-term temperature prediction for the circulation medium

The operating condition of the heat exchange rate (HER) was proposed based on the predicted heat sink temperature in year 50 of operation (i.e., the general lifetime of vertical BHEs). Here, the heat sink temperatures of the GSHP and ASHP refer to the heat pump (HP) inlet and outside air temperatures, respectively. As described in Section 1, intensive GSHP operations, such as daily usage, cause losses in the superior energy performance before reaching the lifetime of the BHE. Therefore, the GSHP was assumed to operate only when the outside temperature was greater than or equal to 34 °C because of the efficiency decrease in the ASHP during the outside temperature rise. According to Bangkok's EnergyPlus weather data, the outside temperature was greater than or equal to 34 °C for 452 h (everyday) and 311 h (weekdays) over the course of a year [24]. The limitation of temperature rise was set to 37 °C for year 50 of operation. A previous study indicated that the GSHP is more energy efficient than the ASHP for heat sink temperature differences of up to +5 °C based on an analysis of experimental data in Bangkok [12]. Herein, we set a permissible temperature difference of up to +3 °C for the heat sink to ensure the long-term superiority of the GSHP to the ASHP. In summary, we proposed an operating condition to the HER that enables a heat sink temperature below 37 °C in year 50.

Using the GSHP to supply hot water could prevent the subsurface temperature from increasing, simultaneously achieving higher efficiency than a gas-fired water heater. The hotel model had a hot water demand for certain activities, such as showers and baths. Hence, only the GSHP for the hotel model was used to supply hot water in addition to cooling operations. Specifically, the GSHP processed 100 kW of cooling load when the outside temperature was greater than or equal to 34 °C, while it extracted 200 kWh of heat/day from the subsurface to generate hot water.

We calculated the annual average heat sink temperature using GroundClub for 10 years after the start of the operation. To reduce the computational load, we estimated the heat sink temperature in year 50 using the first 10 years of operation by extrapolating the approximated temperature curve in the ILS solution. The temperature field of the ILS solution assumes a constant heating amount q/unit depth as follows [32]:

$$T(r,t) = \frac{q}{4\pi\lambda}\int_{\frac{r^2}{4at}}^{\infty}\frac{e^{-u}}{u}du = \frac{q}{4\pi\lambda}E\left(r^2 \Big/ 4at\right), \quad (1)$$

where u is a variable, t is the elapsed time, r is the distance from the ILS, and E is an exponential integral. When $at/r^2 > 20$, E can be approximated as follows, with a maximum error of 2.5%:

$$E\left(r^2 \Big/ 4at\right) = -ln\left(\frac{4at}{r^2}\right) - 0.5772. \quad (2)$$

The ground thermal diffusivity a is denoted as $a = \lambda/c_g$, where λ is the ground thermal conductivity and c_g is the ground specific thermal capacity.

2.2.3. Description of the ground heat exchangers

2.2.3.1. Thermal properties of soil in Bangkok, Thailand. A history matching of the results of the thermal response test using GroundClub was conducted in a previous study for a pilot facility at the Bangkok campus of Chulalongkorn University [12]. The matching parameters were the undisturbed ground temperature, apparent thermal conductivity of the soils, and heat capacity. Apparent thermal conductivity refers to the thermal conductivity of the soil with water flowing in the voids of strata or rocks. Table 4 lists the values of the specific parameters. The lithostratigraphy of

Table 4
Specifications and thermal properties of Bangkok's soil and borehole heat exchangers (BHEs).

Specifications	Value
Soil thermal properties in Bangkok	
Undisturbed temperature of ground (°C)	29.5
Apparent thermal conductivity (W/(m K))	1.82
Heat capacity (kJ/(m^3 K))	2600
Specification and thermal properties of BHE	
Borehole depth (m)	50
Borehole diameter (mm)	150
Backfill material thermal conductivity (W/(m K))	1.8
U-tube pipe outer diameter (mm)	32
U-tube pipe inner diameter (mm)	26
Diagonal distance between center of U-tube pipe (mm)	52
U-tube pipe thermal conductivity (W/(m K))	0.38

the borehole (0–50 m depth) at the pilot facility showed Quaternary lithologic, composed of mainly four layers with gray clay (0–20 m depth), brown sandy clay (20–26 m depth), brown sand with the Bangkok aquifer (26–40 m depth), and medium sand (40–48 m depth) [10]. The typical value in thermal conductivity of Quaternary saturated clay and sand in Japan was 1.43 W/m K, and 1.59 W/m K, respectively [33]. Therefore, the apparent thermal conductivity of the Bangkok site seemed to be enhanced by the aquifer and groundwater flow. This study used these parameters as representative values for the soil thermal properties in Bangkok for the simulation.

2.2.3.2. Specifications of the BHEs. BHEs were embedded to a depth of 50 m based on a subsurface temperature survey of the Chao Phraya Plain [6]. Each BHE had a double U-tube design in which two pairs of U-shaped heat exchange pipes (U-tubes) are inserted in parallel. High-density polyethylene (HDPE), silica sand, and water were used as the U-tube, backfill material, and circulation medium, respectively. Table 4 summarizes the dimensions of the BHEs utilized in the simulation and the thermal conductivities of the silica sand and HDPE.

We arranged the BHE with the specifications listed in Table 4 in a square grid at 5 m intervals for each building model. For the office and hotel, school, and supermarket models, the number of BHEs was 49 (seven rows and seven columns, 7 × 7 hereafter), 98 (7 × 14), and 240 (2 sets, 10 × 12) with total lengths (TL_{BHE}) of 2450 m, 4900 m, and 12,000 m, respectively. Their installed areas were equivalent to 1-, 2-, and 1.5 times the building footprint for the office and hotel, school, and supermarket models, respectively. We disregarded the thermal interaction among each set of BHEs for the supermarket model.

2.3. System modeling and assessment

2.3.1. Target system and boundaries

The target system was a parallel combination of a GSHP and ASHP. We utilized a water-cooled chilling unit as the HP equipment for the GSHP. The energy performance of the target system was evaluated via a comparison with ASHP operation. The system boundaries included the HP equipment of the central air-conditioning system, the chilled water primary pump, and the circulation medium pump. Fig. 2(a) and (b) show the process flow diagram for the central air-conditioning system and system boundaries.

We used the equipment objects in the LCEM tool ver 3.10 to simulate the operation status of the HP, chilled water primary pump, and circulation medium pump at hourly intervals [34,35]. The LCEM tool was developed to simulate the operation status of air-conditioning systems on Excel sheets.[1] The operation status refers to parameters such as power consumption, fuel consumption, and chilled and hot water temperatures, based on inputs such as the outside air conditions, flow rate, and HP inlet temperature. The model in this simulation tool uses equipment-specific formulas based on actual equipment. This study used the most energy-efficient objects for both the water-cooled chilling unit and ASHP (see Fig. B and Table A for details regarding the performance of the HP equipment and object specifications).

2.3.2. Target system simulation

Fig. 3 shows a schematic flow of the three coupled simulation models, DesignBuilder, GroundClub, and the LCEM tool, used to obtain the power consumption of each piece of equipment in the central air-conditioning system.

The hourly averaged flow rate of the circulation medium pump (FR_1) was set such that the temperature difference of the circulation medium (TD_{cm}) at the HP inlet and outlet was within 2 ± 0.1 °C. Meanwhile, the hourly averaged flow rate of the chilled water primary pump (FR_2, FR_3) was set such that the temperature difference of the chilled water (TD_{cw}) at the supply and return was constant at 5 °C (supply: 7 °C, return: 12 °C). The coupled simulation shown in Fig. 3 was performed assuming a constant cooling load processed by the GSHP (CL_{gshp}). CL_{gshp} was set such that the average HER converged to the conditions discussed in Section 2.2.2. The specific calculations involved four steps to obtain the hourly power consumption of each piece of equipment, as well as the *PSR* and *AESR*.

1) Derivation of CL_{gshp}, E_1, and E_3
2) Derivation of E_2 and examination of the agreement in the circulation medium temperatures between GroundClub and LCEM tool
3) Derivation of the power consumption related to the ASHP system (E_4, E_5)
4) Derivation of the *PSR*, annual energy savings (*AES*), and *AESR* from E_1–E_5

2.3.2.1. Derivation of CL_{gshp}, E_1, and E_3. First, we set the constant CL_{gshp} as the cooling load processed by the GSHP. Second, we obtained the chilled water flow rate of the GSHP system (FR_2) by dividing the CL_{gshp} by the specific thermal capacity of water (c_w) and TD_{cw} as follows:

$$FR_2 = \frac{CL_{gshp}}{c_w \cdot TD_{cw}}. \quad (3)$$

Third, the operation status of the GSHP with a given constant CL_{gshp} was simulated using GroundClub. The coefficient of performance[2] (COP) of the water-cooled chilling unit was input into GroundClub as a linear function of the heat sink temperature. The average COP values at load factors of 50%, 60%, 80%, and 100% were used to approximate a linear function of the heat sink temperature, as CL_{gshp} was set such that the load factor of the water-cooled chilling unit did not fall below 50%. The temperatures at the HP inlet (T_{in}), outlet, and FR_1 were obtained. The average HER was calculated for all GSHP operation hours using the following:

$$HER = \frac{CL_{gshp} + E_2}{TL_{BHE}}. \quad (4)$$

Then, we redefined CL_{gshp} as the average HER converged to the conditions described in Section 2.2.2. Finally, the hourly power consumption of the circulation medium pump (E_1) and chilled

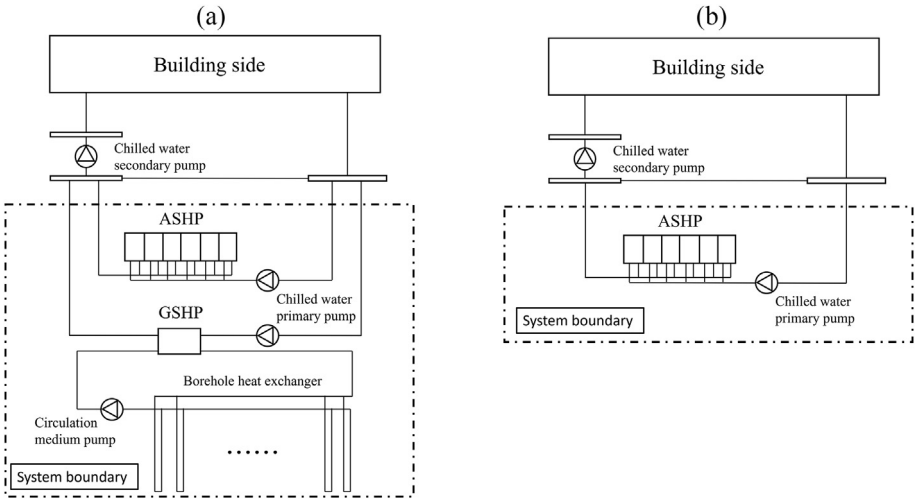

Fig. 2. Process flow diagram for the central air conditioning system and system boundaries.

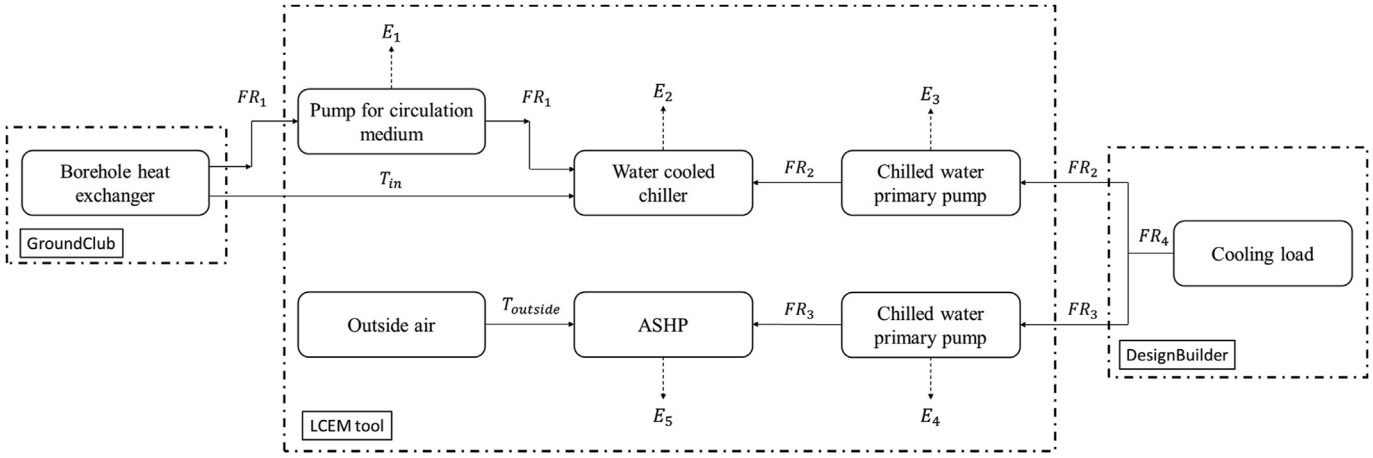

Fig. 3. Schematic flow of the three coupled simulation models
* FR_x: flow rate, E_x: electric power, T_x: temperature.

water primary pump (E_3) were obtained by inputting FR_1 and FR_2, respectively, into the pump objects.

2.3.2.2. Derivation of E_2, and examination of the agreement in the circulation medium temperatures between GroundClub and LCEM tool. We input T_{in}, FR_1, and FR_2 into the water-cooled chilling unit object in the LCEM tool to obtain the power consumption (E_2) and examine whether the average circulation medium temperatures obtained by GroundClub and the LCEM tool matched. The average circulation medium temperature refers to the average of the HP inlet and outlet temperatures. The RMSE reached 0.025 °C, indicating good agreement between the average circulation medium temperatures obtained from GroundClub and the LCEM tool. This demonstrates that the operation statuses of the water-cooled chilling unit were accurately reproduced using the linear function between the COP and heat sink temperature.

2.3.2.3. Derivation of the power consumption of the ASHP system (E_4, E_5). The hourly power consumption of each equipment object of the ASHP system was obtained as follows: First, we obtained FR_4 by dividing the hourly CL obtained using DesignBuilder with c_w and TD_{cw}, which is the hourly averaged flow rate for the chilled water required by the entire central air-conditioning system:

$$FR_4 = \frac{CL}{c_w \cdot TD_{cw}}. \tag{5}$$

Note that FR_4 is the sum of the chilled water flow rates for the GSHP + ASHP system. Second, we obtained FR_3 using Eq. (6), which is the chilled water flow rate for the ASHP system alone.

$$FR_3 = FR_4 - FR_2. \tag{6}$$

Finally, the power consumption of the ASHP (E_5) was obtained by inputting the outside air temperature ($T_{outside}$, retrieved from the EnergyPlus weather data) and FR_3 into the ASHP object. As $FR_4 = FR_3$ when the ASHP is operated alone (i.e., without combination with GSHP), the power consumption of the chilled water primary pump for the ASHP (E_4) was obtained by inputting FR_3 into the objects.

2.3.2.4. Derivation of PSR, AES, and AESR from E_1–E_5. Based on the settings described in Sections 2.3.3.1–3, the power consumption of the GSHP + ASHP system at hour j ($E_{j(gshp+ashp)}$) is expressed as follows:

$$E_{j(gshp+ashp)} = \sum_{i=1}^{5} E_i. \quad (7)$$

Meanwhile, the hourly power consumption of the ASHP-independent system ($E_{j(ashp)}$) is expressed as follows:

$$E_{j(ashp)} = E_4 + E_5. \quad (8)$$

Therefore, the power-saving rate (PSR_j) of the GSHP + ASHP system over the ASHP system can be expressed as follows:

$$PSR_j = \left(1 - \frac{E_{j(gshp+ashp)}}{E_{j(ashp)}}\right) \times 100. \quad (9)$$

The *AES* and *AESR* are expressed on an hourly basis as follows (i.e., 8760 h in a year):

$$AES = \sum_{j=1}^{8760} \left(E_{j(ashp)} - E_{j(gshp+ashp)}\right), \quad (10)$$

$$AESR = \left(1 - \sum_{j=1}^{8760} \frac{E_{j(gshp+ashp)}}{E_{j(ashp)}}\right) \times 100. \quad (11)$$

3. Results

3.1. Cooling loads of the four representative building models

Fig. 4 shows the monthly average cooling loads of the four representative building models described in Section 2.1.

For all the building models, the cooling load tended to be relatively larger from March to July and smaller from November to February. As noted in Fig. A1, Bangkok's outside temperature rises from March to July and falls from November to February. Therefore, the simulation models represent the seasonal fluctuations in the cooling load. The supermarket model exhibited the largest cooling load, followed by the office, school, and hotel models. The differences in the cooling loads are attributable to the differences in the internal heat gain and activity schedule inside each building model.

As shown in Fig. 5, May 17 was used as an example to show the hourly changes in the cooling load for each model. May 17 was selected as its annual maximum outside temperature was 38.5 °C in the EnergyPlus weather data.

The supermarket model showed the largest cooling load during the daytime, owing to its higher heat gain from the equipment and lighting than the other models. The hotel model experienced a decreased internal heat gain and cooling load during the daytime because of the assumed activity schedule. Although the school model had an air-conditioned area less than half that of the office model, the two models had almost the same peak load during the daytime. This is because the occupant density and natural ventilation/occupant are greater for the school model than for the office model, which increased the outside air load. We obtained the average cooling loads of each model by dividing the annual total cooling load by their respective annual business hours. The average cooling loads for the office, school, hotel, and supermarket models were 588.3 kW, 525.4 kW, 436.5 kW, and 728.5 kW, respectively.

3.2. Operating conditions of GSHP system for the representative building models

Fig. 6 presents the average heat sink temperature until year 10 of operation and the extrapolation of the ILS solution in the office model of BHEs, with an average HER of 32.5 W/m.

The average heat sink temperature in the 10th year was 34.9 °C, which is different from 32.9 °C for the same HER in a single BHE with the same specifications and thermal properties. This indicates that there is a faster increase in the heat sink temperature for multiple BHEs than for small-scale systems owing to the thermal interaction between the BHEs. The difference in the temperature rise between the values obtained by the ILS solution and GroundClub was 0.4% (i.e., absolute value of the difference divided by temperature calculated by GroundClub) over years 3–10 of operation. The average heat sink temperature in year 50 was estimated to be 36.8 °C. After confirming that the average heat sink temperature was lower than 37 °C in year 50, we set the average HER to 32.5 W/m as the operating condition for introducing the GSHP in the office model. The operating conditions were also obtained for the other models. Table 5 lists the average HERs for the GSHPs in the building models and the CL_{gshp} values that meet these conditions.

For the school and supermarket models, the heat sink

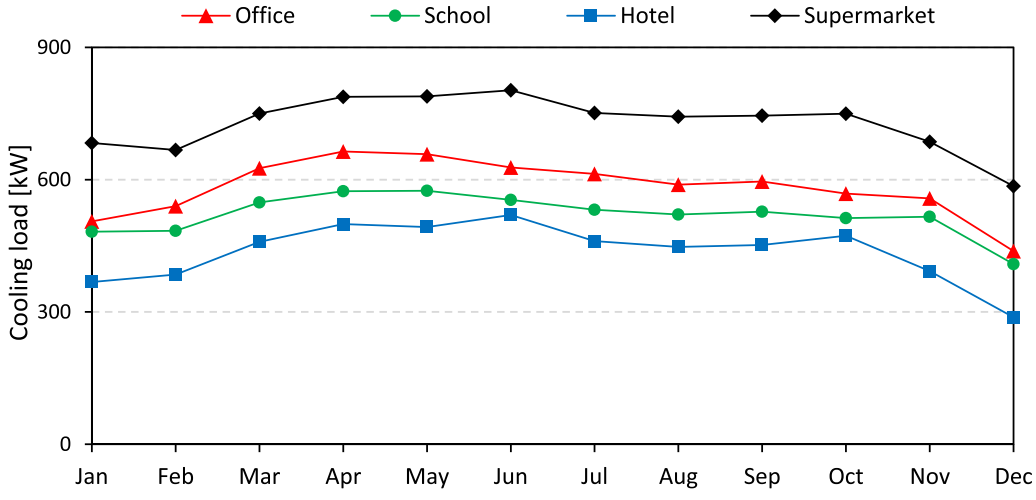

Fig. 4. Monthly averaged cooling loads from hourly data.

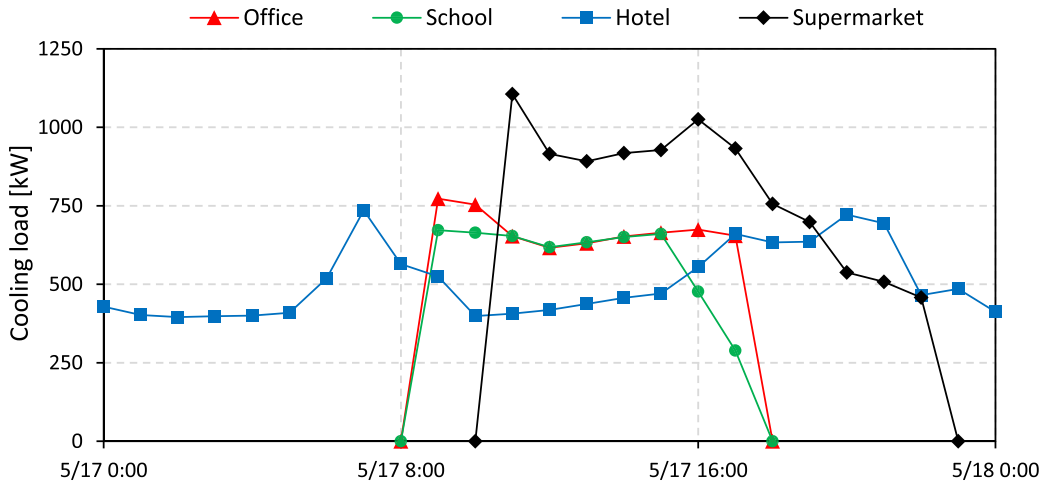

Fig. 5. Cooling load transitions on May 17.

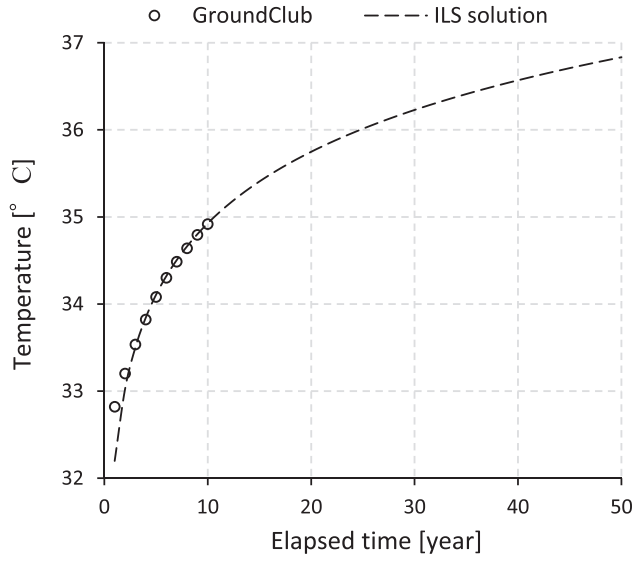

Fig. 6. Extrapolation of the infinite line source (ILS) solution for the office model.

temperature in the 50th year was below 37 °C for the average HERs of 31.0 W/m and 23.5 W/m, respectively, while the temperature rise differences from years 3–10 in the heat sink were 0.3% and 0.6%, respectively. For the hotel model, the heat collected to supply hot water was larger than the dissipation, leading to a continuous decrease in the heat sink temperature. The average heat sink temperature in the 10th year was 32.5 °C, which decreased from 34.3 °C in the first year. The average HER of the supermarket model was 27.7% lower than that of the office model, owing to the longer (by 45%) operating hours of the GSHP in the supermarket model than in the office model.

The heat sink temperature rise reached its average temperature over the 50 years in year 12 for every model except for the hotel model. Further, the difference between the annual average heat sink temperatures in years 10 and 12 was no greater than 0.3 °C. The COP change for the water-cooled chilling unit was approximately 0.04 for a heat sink temperature difference of 0.3 °C at an 80% load factor. Because this change in the COP had little effect on the power consumption, we used the energy performance in year 10 as a reference for the average performance over the lifetime.

Table 6
Energy performance of ground source heat pump (GSHP) + air-source heat pump (ASHP) system for each standard building model.

	Office	School	Supermarket	Hotel
Maximum power-saving rate (*PSR*) (%)	8.7	15.2	19.3	11.8
Average *PSR* (%)	6.7	8.7	19.0	6.4
Annual energy savings (*AES*) (MWh)	3.7	4.5	14.8	3.5
Annual energy-saving rate (*AESR*) (%)	1.2	1.6	2.1	0.5

3.3. Energy performance

Table 6summarizes the maximum and average *PSR*, *AES*, and *AESR* values for the GSHP + ASHP system as compared with the ASHP system under the operating conditions described in Section 2.

The supermarket model had the largest average *PSR* at 19.0%, followed by the school, office, and hotel models at approximately 8.7%, 6.7%, and 6.4%, respectively. These results indicate that the GSHP + ASHP system achieves a higher energy performance than the ASHP system, leading to a reduction in the peak power. The supermarket model had the largest *PSR* among the building models

Table 5
Operating conditions of ground source heat pump (GSHP) systems for each standard building model.

	Office	School	Hotel	Supermarket
Average HER (W/m)	32.5	31.0	47.6	23.5
Average heat injection (kW)	79.6	151.9	116.5	282.0
CL_{gshp} (kW)	67.2	128.3	99.7	237.6
Percentage of CL_{gshp} over the average cooling load (%)	11.4	24.4	22.8	32.6
Annual GSHP operation time (h)	311	311	452	452

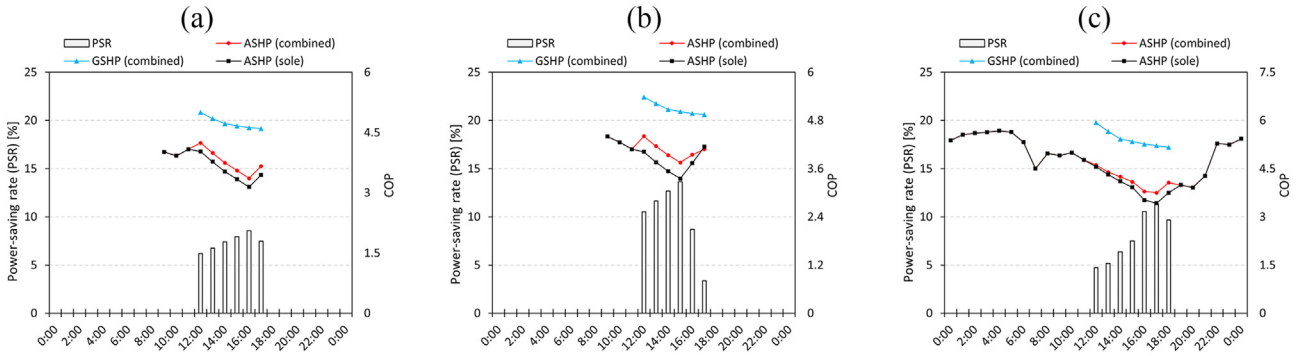

Fig. 7. Hourly changes in power-saving rates (*PSR*s) and coefficient of performance (COP) for the office, school, and hotel models on May 17. *bar graph: *PSR*, line graph: COP.

Table 7
Annual energy savings (*AES*), annual energy-saving rate (*AESR*), and CO_2 emission reduction of ground source heat pump (GSHP) for hot water supply.

	ASHP	Water heater
AES (MWh)	3.94	–
AESR (%)	11.1	–
CO_2 emissions reduction (t-CO_2)	1.96	7.68
CO_2 emissions reduction rate (%)	11.1	32.8

*[11] CO_2 inventory of electricity consumption in Thailand (2019): 0.497 kg − CO_2/kWh [39].
*[22] CO_2 inventory of natural gas combustion (gross calorific value (*GCV*) basis): 56.1 t CO_2/TJ [40].

because it had the largest ground heat exchanger with 240 BHEs, resulting in the largest percentage of CL_{gshp} to the cooling load (almost three times larger than that of the office model). Meanwhile, the average *PSR* values of the school and hotel models were only 30% more than and 5% less than that of the office model, respectively, despite the fact that the percentages of CL_{gshp} to the average cooling loads were almost twice that of the office model. The supermarket model had the largest *AESR* of 2.1%, which was smaller than the *PSR* because the GSHP annual operation hours were significantly lower than the annual business hours of the facility (e.g., 452 h for the GSHP operating hours out of 4380 h for the annual business hours of the supermarket model). The *AES* values of the school and hotel models were not significantly different from that of the office model.

4. Discussion

4.1. Factors affecting energy performance

As described in Section 3.3, the average *PSR* and *AES* values of the school and hotel models were not significantly different from those of the office model, despite their larger percentages of CL_{gshp} to the average cooling loads. To explore the factors that contributed

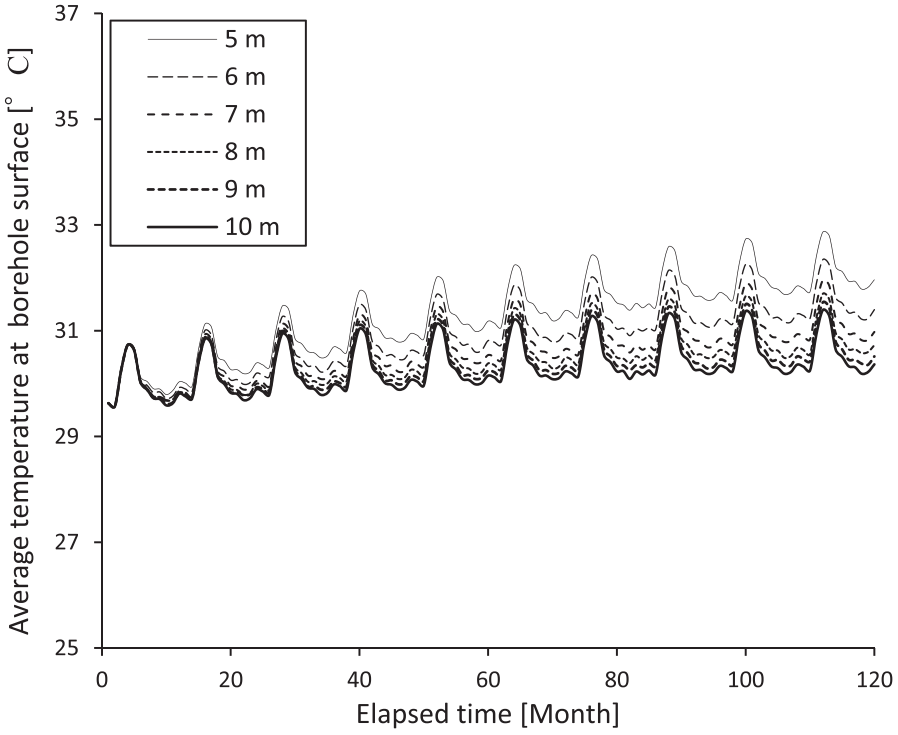

Fig. 8. Monthly average temperatures at the borehole surface with various borehole heat exchanger (BHE) distances.

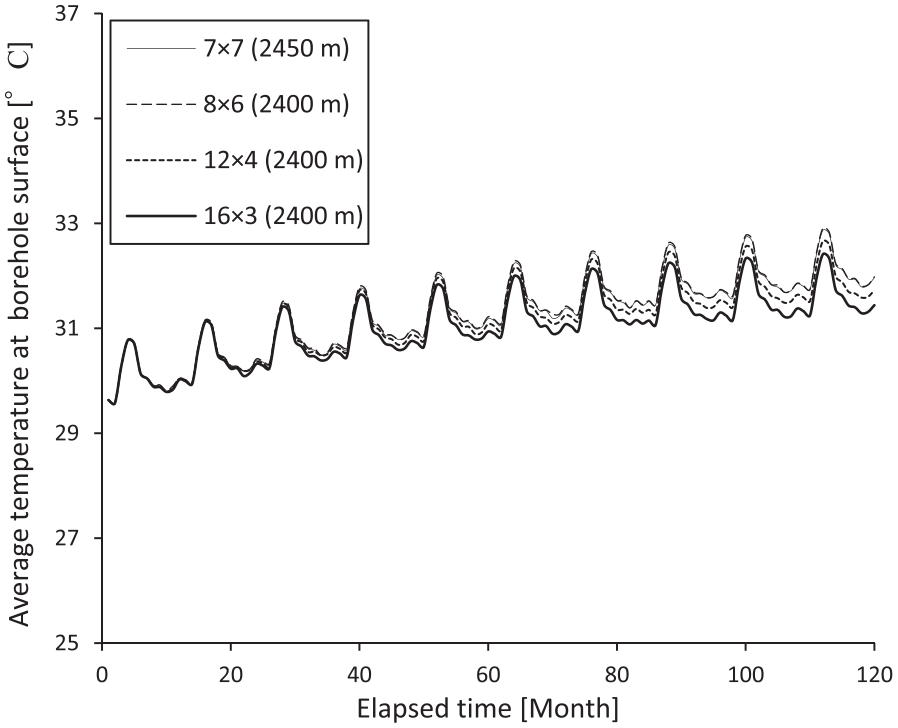

Fig. 9. Monthly average temperatures at the borehole surface with various borehole heat exchanger (BHE) arrangements.

to the suppression of efficiency improvement in these models, we examined the operation statuses, such as the hourly performance in the HP, in more detail. Fig. 7 shows the hourly changes in the *PSR* and COP for the office, school, and hotel models on May 17. On this day, the outside temperature exceeded 34 °C from 11:00 to 18:00 and peaked at 16:00, resulting in GSHP operation from 11:00 to 17:00 for the office and school model, and from 11:00 to 18:00 for the hotel model.

Overall, the GSHP demonstrated 16%–34% higher efficiency than the sole ASHP operation, confirming the consistency with the results from the demo-experiment for small-scale system [10]. While the COP values for both the GSHP and ASHP changed according to the fluctuation of the respective heat sink temperature, those for the ASHP in the combined operation were higher than those in the sole ASHP operation. This is because the COP for the ASHP increased with decreasing load factor in the range of 60%–100% (Fig. B1), implying that the decreased load factor in the ASHP by combined operation improved the *PSR*. Relatively small *PSR*s were observed after 15:00 for the school model and from 11:00 to 15:00 for the hotel model. These small improvements in energy performance are attributable to the decreased cooling loads during these hours. The cooling loads in the school model after 15:00 decreased to approximately 60% of their respective peak loads, as was the case for the hotel model from 10:00 to 15:00 (Fig. 5). Meanwhile, the COP for the ASHP in the range of less than 60% of the load factor was almost constant (Fig. B1), meaning there is little room for improvement in the COP with a decreased load factor by the combined operation. A similar tendency was observed on other days, indicating that the cooling load patterns specific to those models suppress efficiency improvements. These results confirm that within this study's settings, the GSHP maximizes the facilities' energy performance where the cooling load peaks and does not decrease during the daytime.

The largest *AESR* value (2.1%) in this study was lower than those found in previous studies in regions dominated by cooling demand (e.g., 19% and 12.3% for studies in Qatar and Florida, USA, respectively) [15,16]. The significantly low value obtained in this study may be attributable to the difference in the design period and consequent limited operation hours, although differences also exist in the study conditions, such as climate, geology, equipment specifications, and usage patterns. To avoid the risk of overestimating the energy performance of the GSHP in cooling-dominated regions, this difference in performance deserves attention.

4.2. Energy performance of GSHP with the purpose of hot water supply in the hotel model

The GSHP in the hotel model was also used to supply hot water, leading to the extraction of 200 kWh of heat/day from the subsurface. This section examines the *AES*, *AESR*, and CO_2 emission reduction of the GSHP when operated for the purpose of hot water supply in the hotel model over gas-fired water heaters and ASHPs. We assumed that hot water was generated and stored from 0:00 to 5:00, and natural gas was used as the fuel for the heater. Equipment specific data regarding the efficiency (e.g., COP and thermal efficiency) were obtained from the technical data provided by the manufacturer [36–38]. We utilized the COP values for the GSHP and ASHP when T_{in} and $T_{outside} = 25$ °C with a supplied hot water temperature of 65 °C, because the average of T_{in} during the heat extraction in year 10 and that of $T_{outside}$ during 0:00–5:00 were approximately 26 °C. The thermal efficiency of the water heater is

[1] Each piece of equipment (e.g., chiller) is represented by a set of specific formulas. The sets of formulas are input into an Excel sheet. The sets of formulas input into the cells in the sheet are called an "object" in the LCEM tool.

[2] COP refers to the ratio of the processed air-conditioning load to power consumption.

Table A
List of objects and its specifications

	Object name	Specification	Power
1. Office			
Water chilling unit (water-cooled)	RR (CW)-XX1-310H-132	Rated cooling capacity: 118 kW Rated COP: 4.65 (Chilled water: 7–12 °C, HP inlet: 35 °C)	25.4 kW
Pump for circulation medium	PCD(2 P)-XX1-303SI-080_5.5_50	Single suction volute pump (Inverter) Rated performance: 750 L/min	5.5 kW
Chilled water primary pump (GSHP)	PCH(4 P)-XX1-303SI-050_2.2_50	Single suction volute pump (Inverter) Rated performance: 208 L/min	2.2 kW
Air source heat pump (ASHP)	RR-XX2-310UH_85	Rated cooling capacity: 680 kW (8 Units) Rated COP: 4.44 (Chilled water: 7–12 °C, Outside air: 30 °C)	153.0 kW
Chilled water primary pump (ASHP)	PCH(4 P)-XX1-303SI-150_22_50	Single suction volute pump (Inverter) Rated performance: 3335 L/min	22 kW
2. School			
Water chilling unit (water-cooled)	RR (CW)-XX1-310H-170	Rated cooling capacity: 150 kW Rated COP: 5.02 (Chilled water: 7–12 °C, HP inlet: 35 °C)	29.9 kW
Pump for circulation medium	PCD(4 P)-XX1-303SI-100_11_50	Single suction volute pump (Inverter) Rated performance: 1300 L/min	11 kW
Chilled water primary pump (GSHP)	PCH(4 P)-XX1-303SI-065_3.7_50	Single suction volute pump (Inverter) Rated performance: 416.5 L/min	3.7 kW
Air source heat pump (ASHP)	RR-XX2-310UH_85	Rated cooling capacity: 680 kW (8 Units) Rated COP: 4.44 (Chilled water: 7–12 °C, Outside air: 30 °C)	153.0 kW
Chilled water primary pump (ASHP)	PCH(4 P)-XX1-303SI-150_22_50	Single suction volute pump (Inverter) Rated performance: 3335 L/min	22 kW
3. Supermarket			
Water chilling unit (water-cooled)	RR (CW)-XX1-310H-170	Rated cooling capacity: 300 kW (2 Units) Rated COP: 5.02 (Chilled water: 7–12 °C, HP inlet: 35 °C)	59.8 kW
Pump for circulation medium	PCD(4 P)-XX1-303SI-100_11_50	Single suction volute pump (Inv., 2 Units) Rated performance: 2600 L/min	22 kW
Chilled water primary pump (GSHP)	PCH(4 P)-XX1-303SI-065_3.7_50	Single suction volute pump (Inv., 2 Units) Rated performance: 833 L/min	7.4 kW
Air source heat pump (ASHP)	RR-XX2-310UH_85	Rated cooling capacity: 1020 kW (12 Units) Rated COP: 4.44 (Chilled water: 7–12 °C, Outside air: 30 °C)	229.4 kW
Chilled water primary pump (ASHP)	PCH(4 P)-XX1-303SI-150_22_50	Single suction volute pump (Inverter) Rated performance: 3335 L/min	22 kW
4. Hotel			
Water chilling unit (water-cooled)	RR (CW)-XX1-310H-170	Rated cooling capacity: 150 kW Rated COP: 5.02 (Chilled water: 7–12 °C, HP inlet: 35 °C)	29.9 kW
Pump for circulation medium	PCD(2 P)-XX1-303SI-080_5.5_50	Single suction volute pump (Inverter) Rated performance: 750 L/min	5.5 kW
Chilled water primary pump (GSHP)	PCH(2 P)-XX1-303SI-050_2.2_50	Single suction volute pump (Inverter) Rated performance: 197.5 L/min	2.2 kW
Air source heat pump (ASHP)	RR-XX2-310UH_85	Rated cooling capacity: 680 kW (8 Units) Rated COP: 4.44 (Chilled water: 7–12 °C, Outside air: 30 °C)	153.0 kW
Chilled water primary pump (ASHP)	PCH(4 P)-XX1-303SI-150_22_50	Single suction volute pump (Inverter) Rated performance: 3335 L/min	22 kW

Table B
List of hot water equipment and its specifications

	Specification
Hot water heat pump (water source, GSHP)	Heating capacity: 65 kW COP: 3.33 (Hot water: 65 °C, HP inlet: 25 °C)
Hot water heat pump (ASHP)	Heating capacity: 67.7 kW COP: 2.93 (Hot water: 65 °C, Outside air: 25 °C)
Heater (natural gas fired)	Efficiency (gross calorific value basis): 81% Gross calorific value of natural gas: 36.4 MJ/m^3

based on the gross calorific value (*GCV*). Table B details the specifications of the hot-water equipment. The heating load (*HL*) was obtained as follows:

$$HL = 200\,kWh \times \frac{COP_{gshp}}{COP_{gshp} - 1}. \quad (12)$$

The energy consumption rates of the HP and water heater were

obtained by dividing *HL* by the COP and thermal efficiency. Table 7 lists the *AES*, *AESR*, and CO_2 emission reduction of the GSHP for hot water supply.

The *AESR* was 11.1% over the ASHP, and the CO_2 emission reduction rates were 11.1% and 32.8% over the ASHP and water heater, respectively. This indicates that the hot water supply by the GSHP substantially contributed to energy saving and greenhouse gas emission reduction. Therefore, a facility such as a hotel, which has both cooling and hot water demands, will have better energy and environmental performance than those without hot water demand.

4.3. Approaches for further improving energy performance

As detailed in Section 4.2, GSHPs in the tropics have large energy-saving performances when processing both cooling and hot water demand. However, not all facilities have a hot water demand, especially in tropical climates. For a facility without hot water demand, further improvements in energy-saving performance can be reached by increasing the annual operation hours of the GSHP while suppressing the long-term rise in subsurface temperature. A practical approach would be to increase the distance between the BHEs and alter the arrangement of the BHEs to mitigate their thermal interaction. Figs. 8 and 9 show the increase in monthly average temperature at the borehole surface with various distances between BHEs and arrangements of BHEs, using the same conditions as the office model.

The average temperature during the same elapsed time decreased with increasing distance between the BHEs and with increasing slenderness in the arrangement. The degree of decline decayed by more than 7 m in regard to distance, indicating that the recommended distance among the BHEs is at least 7 m in tropical regions. This implies that two approaches, that is, increasing the distance between the BHEs and the slenderness in arrangement, increase the annual operation hours without decreasing the HER. As this study employed a distance of 5 m between the BHEs and a square arrangement shape, further improvements in energy performance are expected by implementing these two approaches. Therefore, further investigation is required to find the optimum combination between the BHE installation area of the site and the arrangement of BHEs, which maximize energy performance.

5. Conclusions

In this study, the potential of subsurface utilization in tropical regions as a heat sink for large-scale GSHP systems was evaluated in terms of energy performance. The *PSR* and *AESR* values for large-scale GSHPs in combination with an ASHP system (hybrid GSHP system) were investigated for four types of commercial building models in Bangkok, Thailand. The energy consumption of the ASHP system was used as the reference performance for a conventional cooling system. The operating conditions of the annual operating hours and heat exchange rate of the GSHP system were set based on the predicted heat sink temperature over the lifetime. The findings of this study are as follows:

- The GSHP operation achieved an average *PSR* of 6%–19%, owing to the high efficiency of the GSHP system and efficiency improvements in the ASHP system with decreased load factor by combined operation.
- An *AESR* of 0.5%–2.1% was achieved, which is significantly lower than that of the *PSR*. This rate is attributable to the fact that the operating conditions limited the GSHP annual operation hours to be significantly lower than the annual business hours of the facility.
- Using the GSHP to supply hot water in the hotel model achieved an *AESR* value of 11.1% over the ASHP and realized annual CO_2 emission reduction rates of 11.1% and 32.8% over the ASHP and gas-fired water heater, respectively. This indicates that the hot water supply by the GSHP has a substantial contribution to energy saving and greenhouse gas emission reductions.

In summary, GSHPs in tropical regions can perform higher efficiency than conventional ASHP systems under operating conditions based on the predicted heat sink temperature over the lifetime. However, owing to load imbalances and high subsurface temperatures, imposing limitations on the annual GSHP operation hours is essential, consequent low *AESRs*, unless the GSHP is used to generate hot water. In this case, the payback period for recovering the initial cost of the hybrid GSHP system may be longer than the conventional system. Further improvements in energy-saving performance can be achieved by mitigating the thermal interaction between the BHEs in order to increase the annual GSHP operation hours. A practical approach would be to increase the distance between the BHEs and the slenderness in their arrangement. Therefore, further research is recommended to identify the optimum combination between the area of the site for BHE installation and the arrangement of BHEs, which maximizes the energy performance.

This study used an analytical solution with the apparent thermal conductivity obtained from the thermal response test. The improvement in the value from the saturated soil includes the thermal advection effect by the aquifer and groundwater flow. In the first place, however, the mechanism of thermal advection is different from thermal conduction. The heat was only accumulated, without transporting outside the system in case of the analytical solution for the conductive model. Thus, the obtained results and discussion in this study can be conservative, underestimating the energy performance of GSHPs in tropical regions. Further investigation on regional groundwater flow is recommended to reproduce the advection effects to the simulation model, such as finite element method.

CRediT authorship contribution statement

Yutaro Shimada: Conceptualization, Methodology, Software, Validation, Formal analysis, Investigation, Resources, Data curation, Writing – original draft, Visualization, Funding acquisition. **Koji Tokimatsu:** Conceptualization, Methodology, Validation, Resources, Writing – review & editing, Supervision, Funding acquisition. **Takashi Asawa:** Conceptualization, Methodology, Writing – review & editing, Supervision. **Youhei Uchida:** Conceptualization, Writing – review & editing, Supervision. **Akira Tomigashi:** Conceptualization, Methodology, Validation, Writing – review & editing, Supervision. **Hideaki Kurishima:** Conceptualization, Resources, Writing – review & editing, Supervision.

Declaration of competing interest

The authors declare that they have no known competing financial interests or personal relationships that could have appeared to influence the work reported in this paper.

Acknowledgments

We express our sincere thanks to Prof. Damien David at INSA de Lyon and Prof. Tomohiko Ihara at the University of Tokyo for raising a scientific question and giving an insightful discussion. We also thank Mr. Poj Hansirisawat at TAIST Tokyo Tech for searching for the

official documents regarding Thailand' s Building Energy Code and assisting with translation. This work was supported by JSPS KAKENHI Grant Number JP21J13612.

Appendix

Fig. A. Monthly average highest air temperature, lowest air temperatures and relative humidity in Bangkok

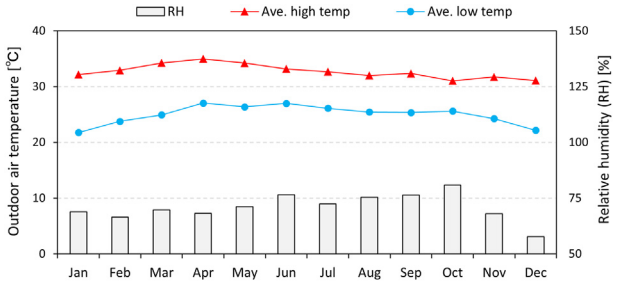

Fig. B. The relationship between the load factor and the coefficient of performance (COP) for the HP equipment

1. ASHP

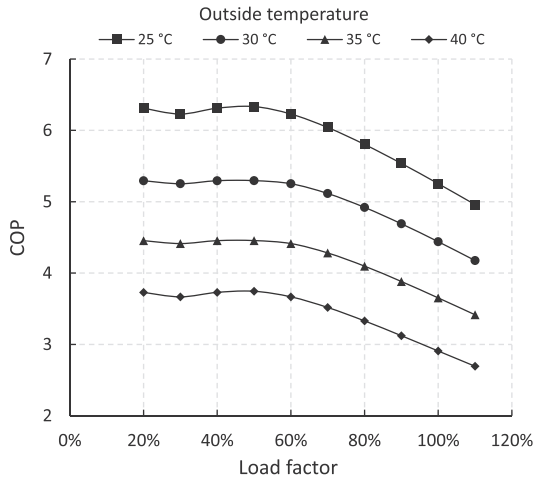

*Note; We used a modular chiller as the ASHP object, whose number of operating modules was controlled by the load factor. This figure shows a case of connection of eight module in a peak.

2. Water-cooled chilling unit

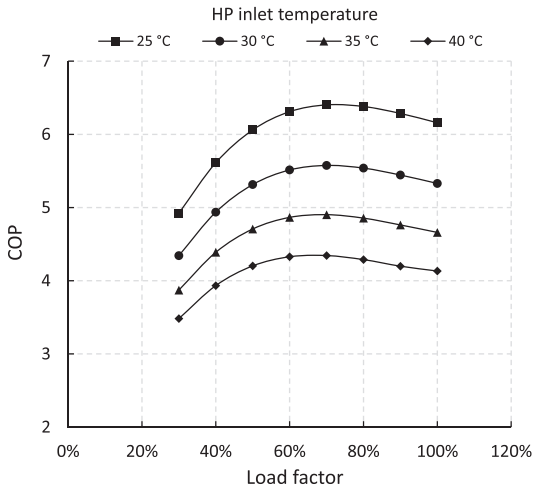

References

[1] IEA, Southeast Asia Energy Outlook 2019, 2019 [Online]. Available, https://www.iea.org/reports/southeast-asia-energy-outlook-2019. Accessed on 21st, October, 2020.
[2] A.S. Haehnlein, P. Bayer, P. Blum, International legal status of the use of shallow geothermal energy, Renew. Sustain. Energy Rev. 14 (9) (2010) 2611–2625, https://doi.org/10.1016/j.rser.2010.07.069.
[3] M. Ouzzane, P. Eslami-Nejad, M. Badache, Z. Aidoun, New correlations for the prediction of the undisturbed ground temperature, Geothermics 53 (2015) 379–384, https://doi.org/10.1016/j.geothermics.2014.08.001.
[4] M. Sasada, S. Takasugi, M. Tateno, A ground source heat pump system in central Tokyo; A case study of retrofit for a small office building, Journal of the Japan Society of Engineering Geology 51 (6) (2011) 265–272, https://doi.org/10.5110/jjseg.51.265, in Japanese.
[5] D. Roy, T. Chakraborty, D. Basu, B. Bhattacharjee, Feasibility and performance of ground source heat pump systems for commercial applications in tropical and subtropical climates, Renew. Energy 152 (2020) 467–483, https://doi.org/10.1016/j.renene.2020.01.058.
[6] K. Yasukawa, et al., Groundwater temperature survey for geothermal heat pump application in tropical Asia, Bull. Geol. Surv. Jpn. 60 (9–10) (2009) 459–467, https://doi.org/10.9795/bullgsj.60.459.
[7] K. Yasukawa, I. Takashima, Y. Uchida, N. Tenma, O. Lorphensri, Geothermal heat pump application for space cooling in Kamphaengphet, Thailand, Bull. Geol. Surv. Jpn. 60 (9–10) (2009) 491–501, https://doi.org/10.9795/bullgsj.60.491.
[8] N. Tenma, K. Yasukawa, I. Takashima, Y. Uchida, O. Lorphensri, G. Zyvoloski, Subsurface thermal influence of experimental geothermal heat pump system operation for space cooling in Kamphaengphet, Thailand, Bull. Geol. Surv. Jpn. 60 (9–10) (2009) 503–509, https://doi.org/10.9795/bullgsj.60.503.
[9] K. Yasukawa, Y. Uchida, Space cooling by ground source heat pump in tropical asia, in: B.I. Ismail (Ed.), Renewable Geothermal Energy Explorations, IntechOpen, 2018 [Online]. Available, https://www.intechopen.com/books/renewable-geothermal-energy-explorations/space-cooling-by-ground-source-heat-pump-in-tropical-asia. Accessed on 21st, October, 2020.
[10] S. Chokchai, et al., A pilot study on geothermal heat pump (GHP) use for cooling operations, and on GHP site selection in tropical regions based on a case study in Thailand, Energies 11 (9) (2018) 2356, https://doi.org/10.3390/en11092356.
[11] A. Widiatmojo, et al., Ground-source heat pumps with horizontal heat exchangers for space cooling in the hot tropical climate of Thailand, Energies 12 (7) (2019) 1274, https://doi.org/10.3390/en12071274.
[12] Y. Shimada, et al., A study on the operational condition of a ground source heat pump in Bangkok based on a field experiment and simulation, Energies 13 (1) (2020) 274, https://doi.org/10.3390/en13010274.
[13] S. Chirarattananon, J. Taweekun, A technical review of energy conservation programs for commercial and government buildings in Thailand, Energy Convers. Manag. 44 (5) (2003) 743–762, https://doi.org/10.1016/S0196-8904(02)00082-1.
[14] V. Yungchareon, B. Limmeechokchai, Energy analysis of the commercial sector in Thailand: potential savings of selected options in commercial buildings, in: SEE International Conference, Hua Hin, 2004, pp. 496–501.
[15] M. Kharseh, M. Al-Khawaja, M.T. Suleiman, Potential of ground source heat pump systems in cooling-dominated environments: residential buildings,

Geothermics 57 (2015) 104–110, https://doi.org/10.1016/j.geothermics.2015.06.009.
[16] Y. Zhu, Y. Tao, R. Rayegan, A comparison of deterministic and probabilistic life cycle cost analyses of ground source heat pump (GSHP) applications in hot and humid climate, Energy Build. 55 (2012) 312–321, https://doi.org/10.1016/j.enbuild.2012.08.039.
[17] DesignBuilder 2019," Version 5.5.2.007 ed. UK: DesignBuilder Software Limited. https://designbuilder.co.uk/.
[18] S. Chirarattananon, J. Taveekun, An OTTV-based energy estimation model for commercial buildings in Thailand, Energy Build. 36 (7) (2004) 680–689, https://doi.org/10.1016/j.enbuild.2004.01.035.
[19] P. Sertsungnern, P. Chaiwiwatworakul, Development of a performance rating scheme of air-conditioning systems for buildings: a case of Thailand, Energy Procedia 9 (2011) 84–94, https://doi.org/10.1016/j.egypro.2011.09.010.
[20] S. Chirarattananon, P. Chaiwiwatworakul, V.D. Hien, P. Rakkwamsuk, K. Kubaha, Assessment of energy savings from the revised building energy code of Thailand, Energy 35 (4) (2010) 1741–1753, https://doi.org/10.1016/j.energy.2009.12.027.
[21] ASHRAE, Standard 62.1-2019 Ventilation for Acceptable Indoor Air Quality, ASHRAE, Atlanta, 2019 [Online]. Available, https://www.ashrae.org/technical-resources/standards-and-guidelines/read-only-versions-of-ashrae-standards. Accessed on 21st, October, 2020.
[22] ASHRAE, Standard 55-2017 Thermal Environmental Conditions for Human Occupancy, ASHRAE, Atlanta, 2017 [Online]. Available, https://www.ashrae.org/technical-resources/standards-and-guidelines/read-only-versions-of-ashrae-standards. Accessed on 22nd, October, 2020.
[23] D.B. Crawley, et al., EnergyPlus: creating a new-generation building energy simulation program, Energy Build. 33 (4) (2001) 319–331, https://doi.org/10.1016/S0378-7788(00)00114-6.
[24] The National Renewable Energy Laboratory (NREL). Weather data. Available: https://energyplus.net/weather. Accessed on 22nd, October, 2020.
[25] ASHRAE, in: International Weather for Energy Calculations (IWEC Weather Files) User Manual and CD-ROM, ASHRAE, Atlanta, 2001. ASHRAE, https://energyplus.net/weather/sources#IWEC. Accessed on 22nd, October, 2020.
[26] K. Nagano, T. Katsura, S. Takeda, Development of a design and performance prediction tool for the ground source heat pump system, Appl. Therm. Eng. 26 (14–15) (2006) 1578–1592, https://doi.org/10.1016/j.applthermaleng.2005.12.003.
[27] T. Katsura, K. Nagano, S. Takeda, Method of calculation of the ground temperature for multiple ground heat exchangers, Appl. Therm. Eng. 28 (14–15) (2008) 1995–2004, https://doi.org/10.1016/j.applthermaleng.2007.12.013.
[28] T. Katsura, K. Nagano, S. Narita, S. Takeda, Y. Nakamura, A. Okamoto, Calculation algorithm of the temperatures for pipe arrangement of multiple ground heat exchangers, Appl. Therm. Eng. 29 (5–6) (2009) 906–919, https://doi.org/10.1016/j.applthermaleng.2008.04.026.
[29] L.R. Ingersoll, O.J. Zabel, A.C. Ingersoll, Heat Conduction with Engineering, Geological, and Other Applications, McGraw-Hill, New York, 1954.
[30] L. Ingersoll, H. Plass, Theory of the ground pipe source for the heat pump, ASHVE Transactions 54 (1948) 339–348.
[31] T. Katsura, K. Nagano, Simulation tool for ground-source heat pump system with multiple ground heat exchangers, in: 2018 Annual Conference, 124, ASHRAE, Houston, 2018, pp. 92–101, no. 2, https://www.techstreet.com/ashrae/standards/ho-18-010-simulation-tool-for-ground-source-heat-pump-system-with-multiple-ground-heat-exchangers?product_id=2024886#full. Accessed on 27th, August, 2020.
[32] S. Gehlin, Thermal Response Test: Method Development and Evaluation 39, Doctoral, Deapartment of Environmental Engineering, Luleå tekniska universitet, Luleå, 2002, 2002, http://www.diva-portal.org/smash/record.jsf?pid=diva2%3A991442&dswid=1416, 27th, August, 2020.
[33] Y. Sakata, T. Katsura, K. Nagano, Estimation of ground thermal conductivity through indicator kriging: nation-scale application and vertical profile analysis in Japan, Geothermics 88 (2020), https://doi.org/10.1016/j.geothermics.2020.101881, 101881.
[34] Ministry of Land, Infrastructure, Transport and tourism. Life cycle energy management (LCEM). (in Japanese) Available: https://www.mlit.go.jp/gobuild/sesaku_lcem_lcem.html. Accessed on 22nd, October, 2020.
[35] M. Ito, et al., Development of HVAC system simulation tool for life cycle energy management Part 1: concept of life cycle energy management and outline of the developed simulation tool, Building Simulation 1 (2) (2008) 178–191, https://doi.org/10.1007/s12273-008-8209-6.
[36] Mitsubishi Electric Corporation. Equipment specific data of hot water heat pump (CRHV-P650A). (in Japanese) Available: https://dl.mitsubishielectric.co.jp/dl/ldg/wink/ssl/wink_doc/m_contents/wink/W_TEC/wyn482036b.pdf. Accessed on 20th, April, 2021.
[37] Mitsubishi Electric Corporation. Equipment specific data of hot water heat pump (CAHV-P500AK2-H). (in Japanese) Available: https://dl.mitsubishielectric.co.jp/dl/ldg/wink/ssl/wink_doc/m_contents/wink/W_TEC/wyn482016.pdf. Accessed on 20th, April, 2021.
[38] Showa Manufacturing Co., Ltd. Equipment specific data of water heater (NEOS-S-1000M). (in Japanese) Available: https://www.showa.co.jp/dcms_media/other/NEOS.pdf. Accessed on 20th, April, 2021.
[39] Energy policy and planning office. CO2 emission per kWh. Available: http://www.eppo.go.th/index.php/en/en-energystatistics/co2-statistic. Accessed on 20th, April, 2021.
[40] IPCC, 2006 IPCC Guidelines for National Greenhouse Gas Inventories Volume 2 Energy Chapter 2 Stationary Combustion, 2006. [Online]. Available: https://www.ipcc-nggip.iges.or.jp/public/2006gl/pdf/2_Volume2/V2_2_Ch2_Stationary_Combustion.pdf. Accessed on 20th, April, 2021.